Desalination and Water Treatment
www.deswater.com

doi:10.5004/dwt.2019.24168

159 (2019) 356–364
August

Photo-catalytic degradation of methylene blue in aqueous solution using TiO_2 supported on bovine bone powder by-product

A. Salhi[a,*], S. Tahiri[a], L. Khamliche[b], A. Aarfane[a], A. Jouali[a], M. Bensitel[c], M. El Krati[a]

[a]*Laboratory of Water and Environment, Department of Chemistry, Faculty of Sciences, University Chouaïb Doukkali, PO. Box 20, El Jadida24000, Morocco, Tel. +21-252-3342325, email: anassalhi@hotmail.com (A. Salhi), tahiri.s@ucd.ac.ma (S. Tahiri), aaarfane@yahoo.com (A. Aarfane), abdelhadi.jouali@gmail.com (A. Jouali), elkrati1@yahoo.fr (M. El Krati)*
[b]*Laboratory of Organic Chemistry, Biochemistry and Environment, Department of Chemistry, Faculty of Sciences, University Chouaïb Doukkali, PO. Box 20, El Jadida24000, Morocco, Tel. +21-252-3342325, email: khamliche@yahoo.fr (L. Khamliche)*
[c]*Laboratory of Catalysis and Corrosion of Materials, Department of Chemistry, Faculty of Sciences, University Chouaïb Doukkali, PO. Box 20 El Jadida24000, Morocco, Tel. +21-252-3342325, email: mbensitel@yahoo.fr (M. Bensitel)*

Received 15 August 2018; Accepted 21 March 2019

ABSTRACT

In this work, TiO_2 supported on bovine bone powder by-product (BBP) was used as photo-catalyst for the degradation of methylene blue (MB) dye in aqueous solutions under UV-irradiation. The main parameters which govern the photo-catalytic treatment efficiency, such as pH, weight of catalyst added to solution, UV-irradiation period, initial concentration of MB and presence of ethanol have been investigated. The new product, BBP-Ti11%, exhibited a good behavior towards the photochemical degradation of methylene blue mainly in basic medium. Photo-degradation performance is inversely proportional to the initial dye concentration. The photo-degradation kinetics of MB is satisfactorily described by the pseudo-first order reaction kinetic model. On the other hand, photo-degradation experiments carried out under UV-irradiation in the presence of ethanol show a decrease of the photo-catalytic activity of the prepared catalyst. This confirm that the discoloration process is mainly done by the action of free radicals $OH^•$ generated on the surface of BBP-Ti 11%. To the best of our knowledge, this is the first report that describes the use of bovine bone powder by-product as support of TiO_2 for the photochemical oxidation of organic dyes.

Keywords: Bovine bone powder; Titanium dioxide; Photo-degradation; Methylene blue

---

1. Introduction

The development of the industrial activities causes a growing pressure on water resources and leads to an important production of waste waters which are responsible for many damages and impacts. The treatment of liquid effluents is more than ever a priority as well to protect the human health, the environment and to produce water which could be recycled in industries or reused in agriculture. The textile dyeing factories require large quantities of water and generate complex colored effluents which are not biodegradable [1]. Indeed, organic dyes are generally persistent pollutants because of the complexity of their chemical structures [2]. Their concentrations in the effluents should be controlled in order to respect environment norms and legislation on water quality which become more stringent. Different techniques such as adsorption [3], membrane filtration [4–7], coagulation-flocculation [8], etc. can be employed to manage dyeing effluents. Advanced oxidation processes (AOPs) are one of the attractive alternatives to the conventional methods. The peculiarity of these processes is that they can eliminate non-biodegradable organic components and avoid the need to dispose of residual sludge. Their operating principle is based on the generation of hydroxyl radicals which are very reactive.

The development of AOPs and the improvement of their efficiency has nowadays become a main research focus. The activity of certain materials can be improved by

---

*Corresponding author.

1944-3994 / 1944-3986

doping them with an element photo-catalytically active. For example, new porous materials based on TiO_2 pillared montmorillonite were synthesised by Chen et al. [9] and their photo-catalytic performances were evaluated by using methylene blue degradation. Carriazo et al. [10] reported in their work the modification of a mineral clay by the incorporation of TiO_2 (anatase) and iron-TiO_2 species to obtain delaminated solids with photo-catalytic activity under very low intensity UV irradiation. TiO_2 was immobilized on perlite granules by Shavisi et al. [11] and obtained material was applied for ammonia degradation in wastewater. Four bentonites and one diatomite were also used by Rossetto et al. [12] as supports for titanium oxide. All materials obtained showed methylene blue photo-degradation activity. On the other hand, the synthesis, by a sol gel method, of TiO_2-montmorillonite photo-catalysts doped with vanadium and/or carbon was carried out by Chen et al. [13]. The degradation of aqueous sulphorhodamine B on these photo-catalysts was investigated under UV-Vis irradiation.

In our previous work, calcium deficient hydroxyapatite (HAP) was synthesized and used as support of different amounts of titanium dioxide. The performance of elaborated material in photo-catalytic degradation of methylene blue dye was then demonstrated [14]. Several research works revealed that bone have a chemical composition similar to that of hydroxyapatites [15,16]. For this reason, the preparation of a new photo-catalyst based on titanium dioxide supported by bovine bone powder by-product (BBP) and its application in photo-degradation will be the subject of this research study. The interest is twofold: (i) First, the elaboration of a composite material which is potentially active and useful for photo-degradation processes. (ii) Second, the valuation of a solid bio-waste, namely bovine bone which is a potential source of hydroxoapatite.

2. Experimental

2.1. Studied dye

Methylene blue (CI 52015) was chosen as a model substance in order to study the photo-catalytic efficiency of bovine bone powder by-product doped with titanium (BBP-Ti11%). It is a heterocyclic aromatic chemical compound (Fig. 1) with the molecular formula $C_{16}H_{18}N_3SCl$ corresponding to a molecular weight of 319.7 g·mol^{-1}. It is a cationic dye molecule belonging to the Xanthines family. Its wavelength of maximum absorption is 664 nm.

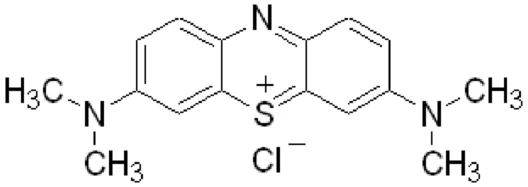

Fig. 1. Chemical structure of methylene blue dye.

2.2. Preparation of TiO_2/bone powder photo-catalyst

Bovine bones were collected from a butcher's shop in El Jadida (Morocco). After cleaning, they were dried at 105°C during 24 h, crushed to smaller pieces of about 1 cm^3, calcined during 6 h at 850°C and then milled by means of a mortar.

A definite amount of the material prepared was impregnated with titanium (IV) isopropoxide $Ti(OiPr)_4$ so as to have a catalyst with 11% of titanium (BBP-Ti11%). The mixture was calcined at 550°C during 4 h and 30 min.

2.3. Characterization of materials

Morphological characterization and chemical composition of the powder materials, BBP and BBP-Ti 11%, were performed using scanning electron microscope Hitachi S-3400N equipped with an energy dispersive X-ray spectroscope (EDS) (Noran with a silicon drift detector). The energy of the acceleration beam employed was 10 kV. Prior to analysis, the sample was carbon coated with a Bal-Tec SCD005 sputter coater.

The size of the particles in the BBP-Ti 11% sample was studied by transmission electron microscopy (TEM; Tecnai G2 12 TWIN FEI operating at 120 kV). For TEM studies, samples were dispersed and deposited on a TEM grid.

Powder materials were also characterized by X-ray diffraction (XRD) using a Bruker AXS D8 Advance diffractometer with Cu Kα radiation (λ = 1.5418 Å). Phase verification was carried out using the EVA software.

IR spectra were recorded using a Tensor 27 FTIR spectrometer from Bruker (Karlsruhe, Germany) equipped with a DLaTGS detector. Spectra were obtained by coadding 50 scans at a resolution of 4 cm^{-1} and a scanner velocity of 10 kHz HeNe frequency, from 4000 to 550 cm^{-1}. For instrumental and measurement control, spectra treatment and data manipulation, it was employed the OPUS program (version 6.5) from Bruker. Spectra recorded are the average of 3 spectra of each sample with a smoothing of 18 points.

The specific surface area of the raw bovine bone powder (BBP) and that doped by titanium (BBP-Ti 11%) have been determined by the Brunauer-Emmett-Teller (BET) method using a Micromeritics ASAP2020 Analyzer.

In order to determine the crystalline form of TiO_2 in the elaborated catalyst (BBP-Ti 11%), the Raman spectra was recorded using a Horiba Jobin Yvon Raman Spectrometer "LabRam HR 800-UV".

UV-Visible diffuse reflectance spectroscopy is one of the most optical methods employed for the determination of gap energy Eg. In this work, a UV-Vis spectrophotometer (Agilent Cary 5000) was used for diffuse reflectance measurements in order to establish the optical band gap. The optical absorption was recorded in the 200–800 nm range. The Kubelka-Munk method (Eq. (1)) can be used to determinate *Eg*. It is based on the following equation [17].

$$F(R) = \frac{(1-R)^2}{2R} \tag{1}$$

where *R* is the reflectance and *F(R)* is proportional to the extinction coefficient α.

Eg can be estimated by the use of the general equation [18].

$$\left[F(R) * h\nu\right] = K * \left(h\nu - Eg\right)^n \tag{2}$$

with *h* is the plank's constant (J·s), *K* is the absorption constant, ν is the light frequency and *n* = 2 for an indirect allowed transition.

2.4. Experimental setup and photo-degradation tests

The photo-catalytic reactor, used in this study, is a cylindrical stainless metal (Fig. 2), equipped with 3 UVA lamps and 3 UVB lamps (8 W, λ: 300–450 nm). The solution to be irradiated was introduced in a Pyrex tube placed in the center of the reactor by means of clamp system. At the bottom, the unit is cooled by a fan to prevent evaporation of solution. The homogeneity of the solution is ensured through agitation, using a bubbler which allows also the aeration of the medium to be treated.

To examine the photo-catalytic efficiency of the prepared catalyst (BBP-Ti 11%), 20 mL of methylene blue solution, with a precisely known concentration, are introduced in the Pyrex tube of the photo-reactor in the presence of 10 mg of BBP-Ti 11% (0.5 g/L of solution). First, the mixture was stirred for 30 min in the dark to reach adsorption equilibrium on the solid surface. The mixture was then UV-irradiated and samples were taken every 30 min and centrifuged with a speed of 4000 rpm for 2 min. The absorbance of the solution was then measured at 664 nm, by the use of a spectrophotometer MAPADA V-1200, before being returned to the reactor.

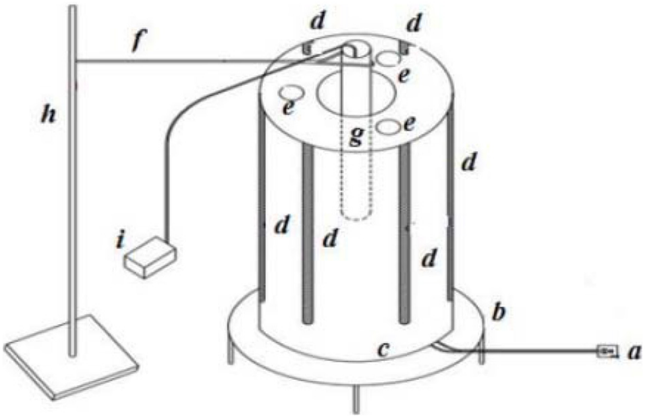

Fig. 2. Simplified scheme of the photoreactor: (a) Power supply cable, (b) Support of reactor, (c) Fan, (d) Lamps, (e) Aeration holes, (f) Clamp, (g) Pyrex tube, (h) Support, and (i) Air bubbler.

3. Results and discussion

3.1. Characterization of the prepared catalyst

Both bovine bone powder by-product (BBP) and prepared catalyst (BBP-Ti11%) were characterized by the scanning electron microscope (SEM) coupled with auxiliary energy dispersive X-ray spectroscopy (EDS). Fig. 3 illustrates the morphological structure of the studied materials which present generally non-uniform and irregular surfaces. The results of the EDS analysis show clearly the presence of titanium in the final synthesized material in addition to the elements mainly present in the bone powder, namely P, Ca, Mg and Na (Fig. 4).

Fig. 5 shows the TEM shots of BBP-Ti11% sample, it is formed of elliptical shaped particles with an average size of 9.9 nm for TiO_2 particles, 16 to 17 nm for calcium particles and about 20 nm for orthophosphates which is the main component of the matrix.

Diffractograms of bovine bone powder (a) and catalyst BBP-Ti 11% (b) show the main characteristic peaks of osse-

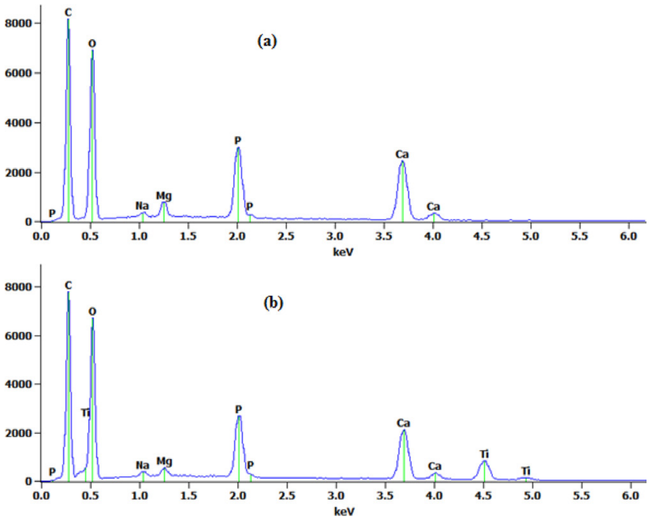

Fig. 4. EDS analysis of raw bone powder BBP (a) and BBP-Ti11% (b).

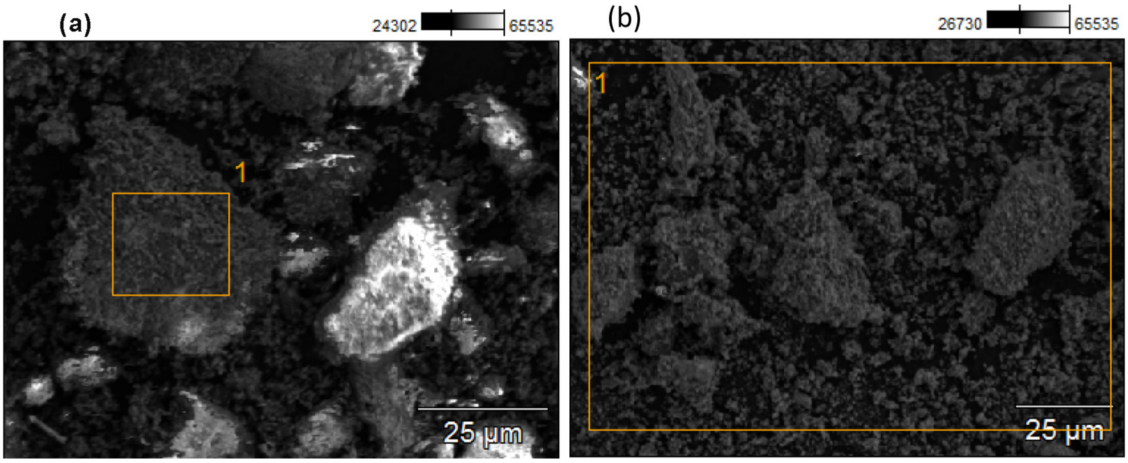

Fig. 3. Scanning electron micrographs of raw bone powder BBP (a) and BBP-Ti11% (b).

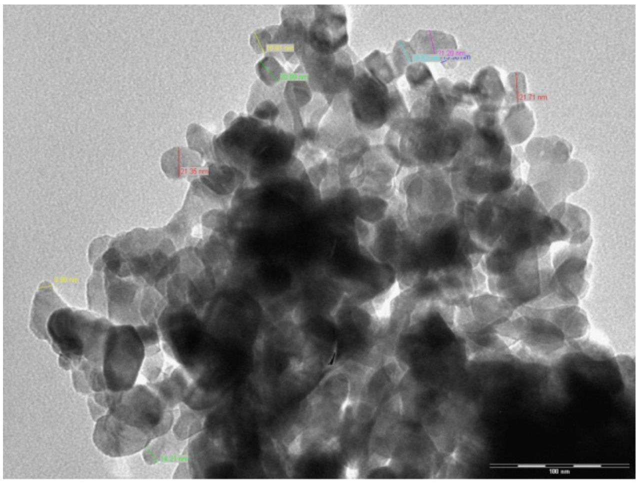

Fig. 5. Transmission electron micrograph of BBP-Ti11%.

ous materials [19,20] and other peaks located at 2-theta (θ) positions 36°, 38°, 46°, 54° and 65° which can be attributed to titanium (Fig. 6). These results are similar to those of our previous work having as objective the preparation of a photo-catalyst TiO_2/hydroxyapatites [21].

The infrared spectra with ATR mode of raw bovine bone powder (BBP) and photo-catalyst (BBP-Ti11%) are shown in Fig. 7. The spectrum related to BBP shows the bands corresponding to the different functional groups present in the bone structure. As can be seen, the band located at 632 cm^{-1} can be attributed to the OH stretching vibration [22]. On the other hand, the bands located at υ_1 962 cm^{-1}, υ_3 1093 and 1034 cm^{-1} and υ_4 604 and 566 cm^{-1} are assigned to PO_4^{3-} [23–27]. The FTIR spectrum corresponding to BBP-Ti11%, presents generally the same shape as that of raw powder (BBP). The main difference is that the spectrum of the prepared catalyst shows a band in the form of a shoulder centered near 750 cm^{-1}. This band can be attributed to Ti-O vibrations and results from doping process.

The BET analysis shows that the bone powder (BBP) has a very low specific surface area (about 0.524 m²/g). However, the impregnation of the powder by titanium improves its specific surface area ($S_{BBP/Ti11\%}$ = 6.32 m²/g).

The Raman spectrum of BBP-Ti11% (Fig. 8) highlights the various absorption bands recorded between 50 and 1400 cm^{-1}. The peaks at about 141, 195, 395, 515 and 636 cm^{-1} confirm the anatase structure of titanium. Similar positions were also obtained in others works for anatase phase [28–30].

The band gap energy of BBP-Ti11% catalyst was obtained by plotting $(F(R)*h\nu)^{1/2}$ as a function of energy ranged from 2 to 4.4 eV (Fig. 9). A straight line was obtained on the linear part between 3.30 and 3.75 eV. The energy of the forbidden band Eg which is equal to 3.22 eV was then determined from linear regression and extrapolation on the x-axis.

3.2. Photo-catalytic activity of the prepared material

The evolution of C/C_0 ratio as a function of time was first studied using three experimental protocols: (i) irradiation of MB solution by UV light without the presence of any material, (ii) irradiation of MB solution by UV light in the presence of bovine bone powder BBP, and (iii) irradiation of MB solution by UV light in the presence of the catalyst ($m_{BBP\text{-}Ti11\%}$ = 0.01 g). From the results shown in Fig. 10, it can be concluded that discoloration of methylene blue solution during eight hours of irradiation, in absence and in presence of the raw bovine bone powder is insignificant and does not exceed 6% and 8%, respectively. On the other hand, and as it can be seen from Fig. 10, BBP-Ti11% catalyst has a very remarkable effect on the discoloration efficiency which reaches about 94% after eight hours of UV irradiation, this confirms the photo-catalytic activity of the aforementioned prepared composite material.

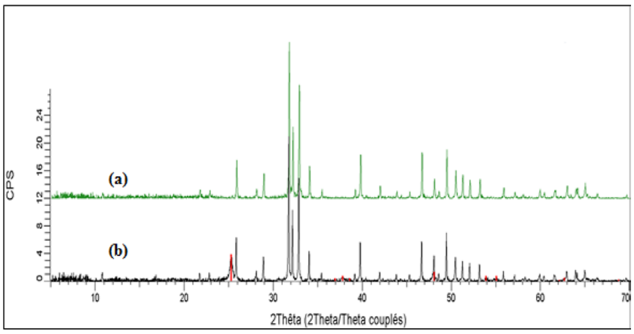

Fig. 6. X-ray diffraction spectra of bovine bone powder BBP (a) and synthesized catalyst BBP-Ti11% (b).

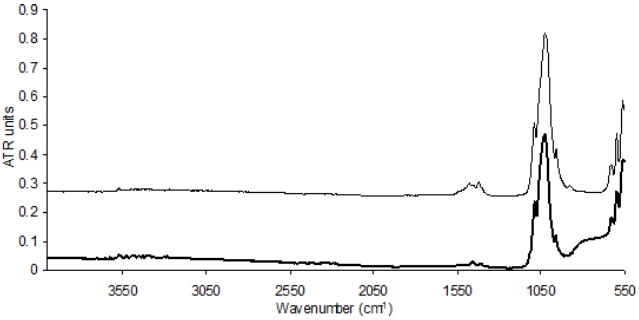

Fig. 7. FTIR spectra of raw bone powder (BBP) and BBP-Ti11% catalyst.

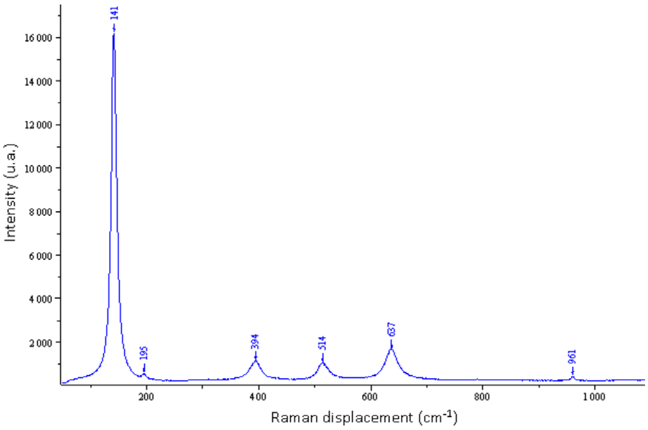

Fig. 8. Raman spectra of BBP-Ti11% catalyst.

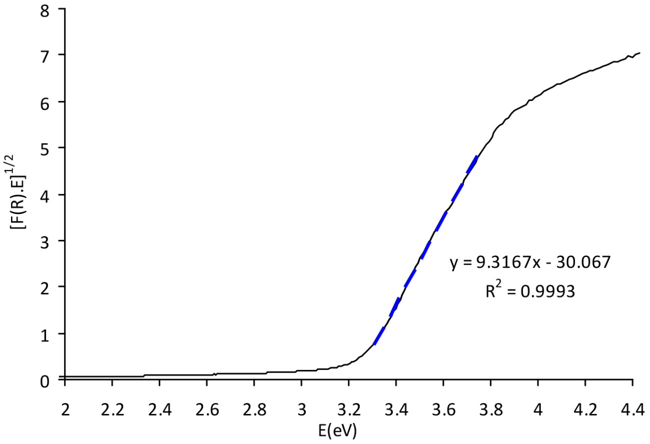

Fig. 9. Graphical representation of modified Kubelka–Munk $[F(R)*h\nu]^{1/2}$ versus E for Eg calculation.

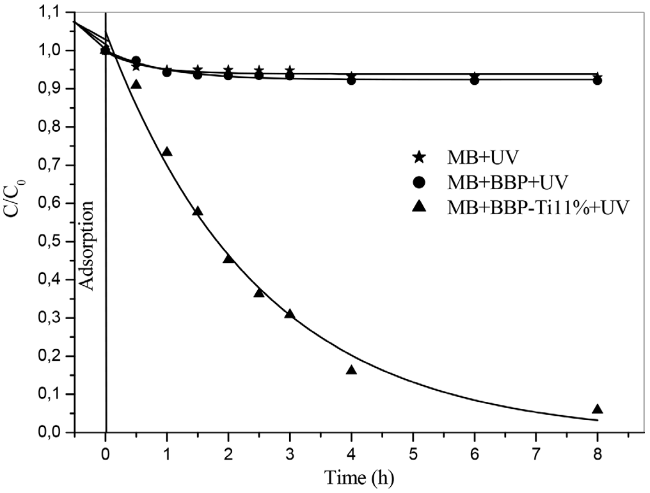

Fig. 10. Effects of UV, BBP+UV and BBP-Ti11%+UV on MB degradation (treated volume: 20 mL; dye concentration: 10 mg/L; BBP or BBP-Ti11%: 0.01 g).

3.3. Effect of pH

The pH of the medium greatly affects the charge on the surface of the catalyst and the size of the aggregates [31], this influences the adsorption of pollutants on the catalyst surface. To study the effect of initial pH on the photo-degradation efficiency, three solutions of MB dye at 10 mg/L were prepared and their pH were adjusted to the desired values by the use of HCl or NaOH solutions. A mass of 0.01 g of the catalyst BBP-Ti 11% was then added to each solution and the mixtures were UV irradiated under the same experimental conditions. After treatment, the solutions were centrifuged and the supernatants were analyzed. The results obtained and presented in Fig. 11 show clearly that photo-degradation of MB dye during 150 min under UV irradiation and in the presence of BBP-Ti 11% is pH dependent. The performance of the process reaches about 64%, 71% and 92% in neutral, acidic and basic solutions, respectively. These results can be explained by the fact that the pH of the aqueous solution greatly affects the surface charge of the catalyst and subsequently influences the adsorption and discoloration performance. Indeed, a number of studies have shown that in aqueous medium and at acidic pH, the titanium dioxide surface is positively charged ($TiOH_2^+$). This promotes the adsorption of anionic molecules by electrostatic attraction. However, the material attracts cationic molecules in basic medium because its surface is charged negatively (TiO^-) [32]. This explains the behavior of methylene blue under the aforementioned operating conditions. The studied dye is cationic in nature, so it will be best adsorbed in basic medium on the photo-catalyst surface [31]. This promotes further the reaction between the dye and the prepared catalyst and improves consequently the discoloration efficiency.

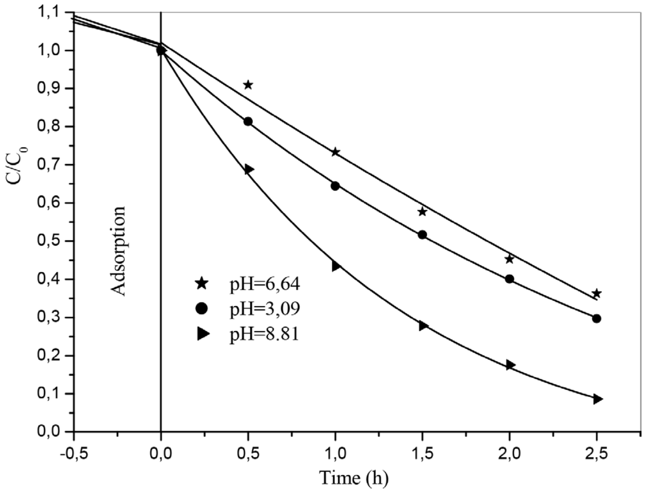

Fig. 11. Photo-degradation of MB solution as a function of pH (treated volume: 20 mL; dye concentration: 10 mg/L; BBP-Ti11%: 0.01 g).

3.4. Effect of the initial dye concentration

The effect of the initial dye concentration on the photo-degradation efficiency was investigated. To optimize this parameter we studied the discoloration of three solutions of MB having three different concentrations (10, 15 and 20 mg/L). It can be seen from Fig. 12 that the increase of the initial dye concentration leads to a decrease of the rate of discoloration. Therefore, photo-degradation performance is inversely proportional to the initial concentration of the solution to be treated. In the presence of BBP-Ti11% and after three hours of UV irradiation, photo-degradation rates are about 28%, 41% and 70% for the studied concentrations 20, 15 and 10 mg/L, respectively. When the dye concentration increases, the amount of dye adsorbed on the catalytic surface also increases. It is clear that this adsorption affects the catalytic activity of TiO_2, supported on the bovine bone powder, and reduces the generation of hydroxyl radicals [33]. Increasing the dye concentration inhibits light access to the entire semiconductor surface. In fact, at high concentration of methylene blue, a significant amount of ultraviolet light can be absorbed by the dye molecules rather than by the catalyst. As the concentration of MB solution increases, the photons get intercepted before they can reach the cat-

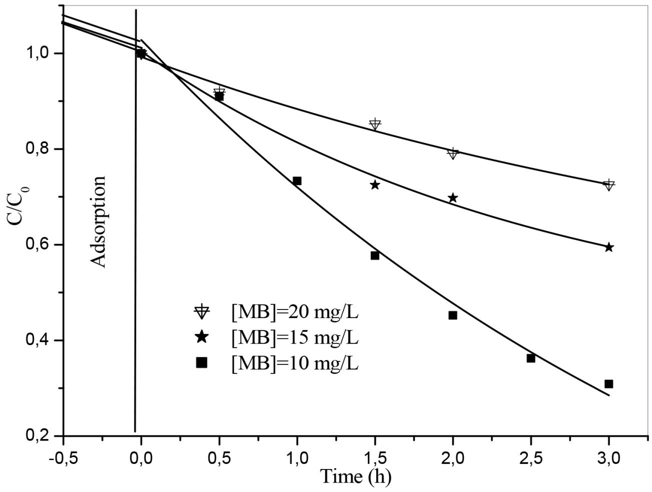

Fig. 12. Effect of initial dye concentration on the discoloration efficiency as a function of time (treated volume: 20 mL; BBP-Ti11%: 0.01 g).

alyst surface. As a result, the catalytic efficiency decreases [33–35]. These findings are consistent with those of other researchers who have studied the photo-degradation of organic dyes [34,36].

3.5. Effect of the irradiation time on visible absorption spectrum of dye

In order to highlight the effect of irradiation time on photo-degradation and determine the optimal time required to reach a total discoloration of MB solution, the evolution of its visible absorption spectrum was monitored during 10 h. The recorded absorption spectra are shown in Fig. 13. As it can be seen, UV-irradiation of MB solution in the presence of BBP-Ti 11% leads to an obvious decrease in the intensity of the absorption spectrum. An irradiation period of about 10 h is more than enough to discolour completely MB solution. As can be seen, we notice a progressive decrease of the maximal absorption band of the studied dye with time until its total disappearance at the end, after ten hours of irradiation. We also find that the rate of decrease is very important during the first two hours of irradiation (reduction of about 55 %). At the end of treatment, the yield of discoloration can reached its highest level (about 96–100%).

3.6. Kinetic of discoloration

The kinetic of discoloration, of methylene blue solutions at various concentrations, was studied. The apparent first-order kinetic rate constant (k_{app}) was calculated from the slope of the linear Eq. (4) which is obtained by integrating Eq. (3).

$$V = \frac{dC}{dt} = k_{app} \cdot C \tag{3}$$

$$Ln\left(\frac{C_0}{C}\right) = k_{app} \cdot t \tag{4}$$

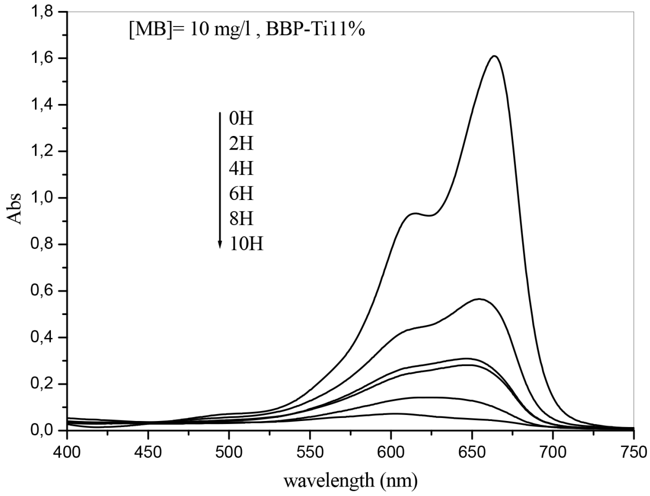

Fig. 13. Evolution of the visible absorption spectrum of MB solution in the presence of BBP-Ti11% (0.01 g) as a function of UV irradiation time (treated volume: 20 mL; dye concentration: 10 mg/L).

Fig. 14 shows the plot of $Ln(C_0/C)$ versus time for three concentrations of MB solution. The constants k_{app} and the coefficients of determination R^2 are presented in Table 1. As it can be seen, the photo-degradation kinetics of MB is satisfactorily described by the pseudo-first order reaction kinetic model. The apparent rate constant k_{app}, however, is very sensitive to initial concentration of dye. It is evident from Table 1 that the reaction rate constant decreases with increasing dye concentration. This can be explained, as has been mentioned, by the reduction of hydroxyl radical generation due to the access inhibition of UV light to the surface of catalyst.

3.7. Effect of ethanol on photo-degradation

Photo-catalytic process may occur according to two routes: the first due to the presence of radicals $OH^•$ and the second due to the positive hole (h^+) formed during UV irradiation of the surface of photo-catalysts [37,38]. To highlight the importance of radicals $OH^•$ in oxidation or photo-oxidation catalytic reactions, alcohols are often used because they act by trapping these radicals. The choice is usually focused on ethanol, isopropanol or t-butanol because of their high reactivity towards hydroxyl radicals [39,40]. In addition, these products do not interact with incident light since they do not absorb beyond 260 nm [41].

In order to reveal the role of radicals $OH^•$ in the photo-catalytic process, the photo-degradation of MB solutions by BBP-Ti11% was monitored as a function of time in the presence and absence of ethanol. The results obtained are summarized in Fig. 15. It is evident from these results that ethanol decreases considerably the photo-catalytic activity of the prepared catalyst BBP-Ti11%. Indeed, after three hours of UV irradiation, the degradation yield of MB dye decreased from 70% in the absence of ethanol to 19% in its presence. Thus, the discoloration process is mainly done by the action of free radicals $OH^•$ generated on the surface of BBP-Ti11%.

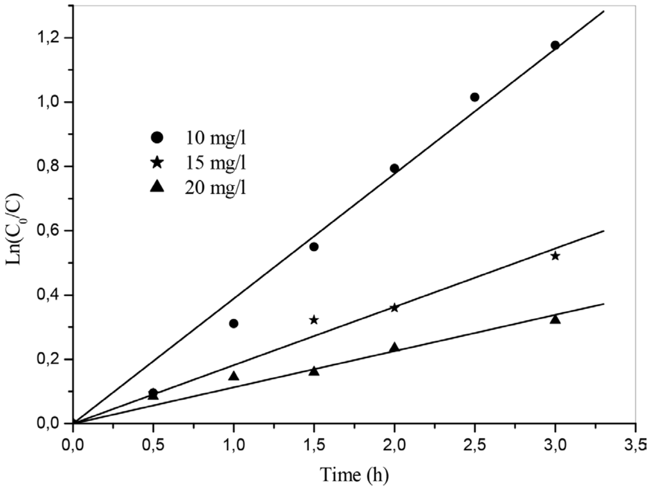

Fig. 14. First-order kinetic plots for photodegradation of MB dye at different initial concentrations (treated volume: 20 mL; BBP-Ti11%: 0.01 g).

Table 1
Apparent first-order kinetic rate constants and time of half reaction for different initial dye concentrations

[MB] (mg/L)	10	15	20
k_{app} (h^{-1})	0.388	0.1815	0.1127
R^2	0.9844	0.9828	0.9637
$t^{1/2}$ (h)	1,78	3,85	6,15

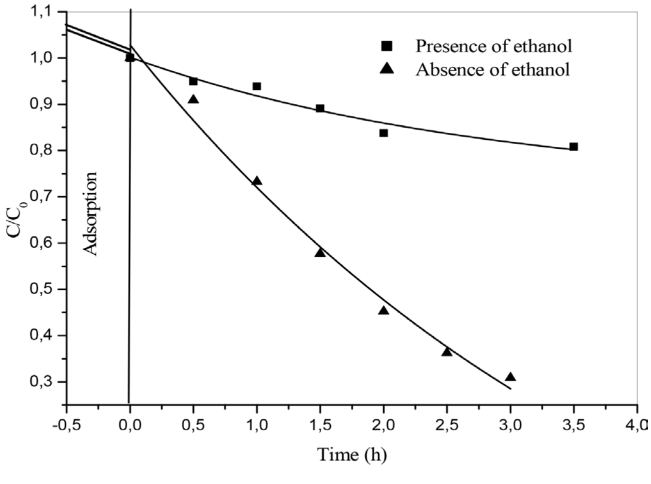

Fig. 15. Effect of the ethanol on the photodegradation of MB dye (treated volume: 20 mL; dye concentration: 10 mg/L; BBP-Ti11%: 0.01 g).

3.8. Effect of catalyst mass

In the case of the heterogeneous catalysis, it is very important to study the effect of the catalyst mass on the speed of discoloration. For that purpose, we conducted experiments by varying the mass of the BBP-Ti11% catalyst from 0.25 g/L until 1.5 g/L. According to the obtained results shown in Fig. 16, we notice that discoloration speed increases with the increase of the catalyst mass (BBP-Ti 11%) and reaches its maximum with a concentration of catalyst of about 1 g/L. Beyond this mass the rate of discoloration decreases because the screening effect becomes dramatic. This reduces penetration of UV light and masks part of the sensitive surface and consequently, degradation efficiency is reduced [42]. A similar phenomenon has also been reported by other authors. Other scientific works showed that the aggregation of particles at high concentrations leads to a reduction in the number of active sites of surface [43].

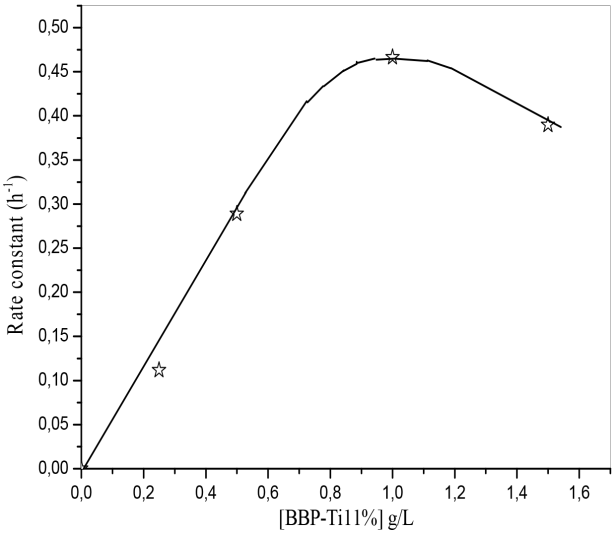

Fig. 16. Evolution of rate constant as a function of catalyst mass (treated volume: 20 mL; dye concentration: 10 mg/L).

4. Conclusion

A new value-added material BBP-Ti11% was elaborated from bovine bone powder by-product (BBP) and titanium (IV) isopropoxide $Ti(OiPr)_4$. This paper reports the applicability of BBP-Ti 11% as new photo-catalyst material which can be applied successfully, under UV-irradiation, in discoloration of MB aqueous solution. The activity of the catalyst seems to be pH dependent; the best efficiency was reached in basic medium. The photo-degradation kinetics follows pseudo-first order chemical kinetics. With the increase in the initial dye concentration, the apparent rate constant is found to decrease significantly. The inhibition of MB photo-degradation by ethanol confirms that the free radicals OH· play an important role in the photo-catalytic reaction. The excessive addition of catalyst decreases the photo-degradation of the dye due to the screening effect that affects the propagation of UV light in the medium.

Acknowledgments

The authors thank Mrs. Nadia Guignard from Institute of Chemistry of Materials and Media of Poitiers (IC2MP) (UMR CNRS 7285) and Professor Rachid Brahmi from Faculty of Sciences of El Jadida for gap energy determination and Raman spectroscopy analysis.

References

[1] N. Guettaî, H. Ait Amar, Photo-catalytic oxidation of methyl orange in presence of titanium dioxide in aqueous suspension. Part I: Parametric study, Desalination, 185 (2005) 427–437.

[2] M. Wang, X. Liu, B. Pan, S. Zhang, Photo-degradation of Acid Orange 7 in a UV/acetylacetone process, Chemosphere, 93 (2013) 2877–2882.

[3] A. Aarfane, A. Salhi, M. El Krati, S. Tahiri, M. Monkade, E.K. Lhadi, M. Bensitel, Kinetic and thermodynamic study of the adsorption of Red195 and Methylene blue dyes on fly ash and bottom ash in aqueous medium, J. Mater. Environ. Sci., 5 (2014) 1927–1939.

[4] A. Majouli, S. Tahiri, S. Alamiyounssi, H. Loukili, A. Albizane, Elaboration of new tubular ceramic membrane from local Moroccan perlite for micro filtration process. Application to treatment of industrial waste waters, Ceram. Int., 38 (2012) 4295–4303.

[5] E. Chahid, H. Loukili, S. Tahiri, S.A. Younssi, A. Majouli, A. Albizane, Filtration of methylene blue, hexavalent chromium, and ethylenediaminetetracetic acid through an ultra-filtration ceramic $ZnAl_2 O_4$ -TiO_2 -based membrane, Water Qual. Res. J. Can., 43 (2008) 313–320.

[6] N. Saffaj, H. Loukili, S.A. Younssi, A. Albizane, M. Bouhria, M. Persin, A. Larbot, Filtration of solution containing heavy metals and dyes by means of ultra filtration membranes deposited on support made of Moroccan clay, Desalination, 168 (2004) 301–306.

[7] V. Buscio, M.J. Marín, M. Crespi, C. Gutiérrez-Bouzán, Reuse of textile waste water after homogenization–decantation treatment coupled to PVDF ultra filtration membranes, Chem. Eng. J., 265 (2015) 122–128.

[8] H.B. Mansour, O. Boughzala, D. Dridi, D. Barillier, L. Chekir-Ghedira, R. Mosrati, Les colorants textiles sources de contamination de l'eau : Criblage de la toxicité et des méthodes de traitement, J. Water Sci., 24 (2011) 209–238.

[9] D. Chen, Q. Zhu, F. Zhou, X. Deng, F. Li, Synthesis and photo-catalytic performances of the TiO_2 pillared montmorillonite, J. Hazard. Mater., 235–236 (2012) 186–193.

[10] J.G. Carriazo, M.M. Forero, R.A. Molina, S. Moreno, Incorporation of titanium and titanium–iron species inside a smectite-type mineral for photo-catalysis, Appl. Clay Sci., 50 (2010) 401–408.

[11] Y. Shavisi, S. Sharifnia, S.N. Hosseini, M.A. Khadivi, application of TiO_2/per lite photo-catalysis for degradation of ammonia in wastewater, J. Ind. Eng. Chem., 20 (2014) 278–283.

[12] E. Rossetto, D.I. Petkowicz, J.H.Z. dos Santos, S.B.C. Pergher, F.G. Penha, Bentonites impregnated with TiO_2 for photo-degradation of methylene blue, Appl. Clay Sci., 48 (2010) 602–606.

[13] K. Chen, J. Li, J. Li, Y. Zhang, W. Wang, Synthesis and characterization of TiO_2–montmorillonites doped with vanadium and/or carbon and their application for the photo-degradation of sulphorhodamine B under UV-vis irradiation, Colloid Surface A: Physicochem. Eng. Aspects, 360 (2010) 47–56.

[14] A. Salhi, A. Aarfane, S. Tahiri, L. Khamliche, M. Bensitel, F. Bentiss, M. El Krati, Study of the photo-catalytic degradation of methylene blue dye using titanium-doped hydroxyapatite, Med. J. Chem., 4 (2015) 59–67.

[15] D. Tadic, M. Epple, A thorough physicochemical characterisation of 14 calcium phosphate-based bone substitution materials in comparison to natural bone, Biomaterials, 25 (2004) 987–994.

[16] M. Figueiredo, J. Henriques, G. Martins, F. Guerra, F. Judas, H. Figueiredo, Physicochemical characterization of biomaterials commonly used in dentistry as bone substitutes-comparison with human bone, J. Biomed. Mater. Res. B., 92 (2009) 409–419.

[17] Q. Li, R.C. Xie, Y.W. Li, E.A. Mintz, J.K. Shang, Enhanced visible-light-induced photo-catalytic disinfection of E.coli by carbon-sensitized nitrogen-doped titanium oxide., Environ. Sci. Technol., 41 (2007) 5050–5056.

[18] R. López, R. Gómez, Band-gap energy estimation from diffuse reflectance measurements on sol–gel and commercial TiO_2: a comparative study, J. Sol-Gel Sci. Technol., 61 (2012) 1–7.

[19] M. El Haddad, R. Slimani, R. Mamouni, S. El Antri, S. Lazar, Removal of two textile dyes from aqueous solutions onto calcined bones, J. Assoc. Arab Univ. Basic Appl. Sci., 14 (2013) 51–59.

[20] G. Ghanizadeh, G. Asgari, Adsorption kinetics and isotherm of methylene blue and its removal from aqueous solution using bone charcoal, J. Reac. Kinet. Mech. Cat., 102 (2011) 127–142.

[21] A. Salhi, A. Aarfane, S. Tahiri, L. Khamliche, M. Bensitel, S. Rafqah, N. Benzidia, M. El Krati, Preparation and photo-catalytic efficiency evaluation of hydroxyapatite – titanium toward orange acid 7 dye in aqueous medium, J. Mater. Environ. Sci., 5 (2014) 1573–1582.

[22] C.C. Ribeiro, I. Gibson, M.A. Barbosa, The uptake of titanium ions by hydroxyapatite particles-structural changes and possible mechanisms, J. Biomater., 27 (2006) 1749–1761.

[23] Y. Leung, M.A. Walters, R.Z. Legeros, Second derivative infrared spectra of apatite, Spectroc. Acta., 46A (1990) 1453–1459.

[24] L.M. Miller, V. Vairavamurthy, M.R. Chance, R. Mendelshon, E.P. Paschalis, F. Betts, A.L. Boskey, In situ analysis of mineral content and crystallinity in bone using infrared micro-spectroscopy of the nu(4) PO_4^{3-} ibration, Biochim. Biophys. Acta, 1527 (2001) 11–19.

[25] B.O. Fowler, Infrared studies of apatites. I. Vibrational assignments for calcium, strontium, and barium hydroxyapatites utilizing isotopic substitution, Inorg. Chem., 13 (1974) 194–207.

[26] B.O. Fowler, E.C. Moreno, W.E. Brown, Infra-red spectra of hydroxyapatite, octacalcium phosphate and pyrolysedoctacalcium phosphate, Arch. Oral. Biol., 11 (1966) 477–492.

[27] C. Rey, M. Shimizu, B. Collins, M.J. Glimcher, Resolution-enhanced Fourier transform infrared spectroscopy study of the environment of phosphate ion in the early deposits of a solid phase of calcium phosphate in bone and enamel and their evolution with age: 2. Investigations in the Nu_3PO_4 domain, Calcif. Tissue Int., 49 (1991) 383–388.

[28] F. Abbas, R. Bensaha, H. Tarore, Effect of Hg^{2+} doping and of the annealing temperature on the nanostructural properties of TiO_2 thin films obtained by sol–gel method, C.R. Chimie, 17 (2014) 1176–1183.

[29] G. Guang-Rui, L. Ying-Ai, T. Yan-Chun, H. Zhi, L. Jun-Jie, Y. Hong, L. Wei-Qin, Z. Yong-Nian, Investigation on the structure of TiO_2 films sputtered on alloy substrates, Vacuum, 71 (2003) 487–490.

[30] N.S. Allena, N. Mahdjoub, V. Vishnyakov, P.J. Kelly, R.J. Kriek, The effect of crystalline phase (anatase, brookite and rutile) and size on the photo-catalytic activity of calcined polymorphic titanium dioxide (TiO_2), Polym. Degrad. Stab., 150 (2018) 31–36.

[31] P.F. Luckham, S. Rossi, The colloidal and rheological properties of bentonite suspension, Adv. Colloid Interf. Sci., 82 (1999) 43–92.

[32] X. Weimin, S.U. Geissen, Separation of titanium dioxide from photo-catalytically treated water by cross-flow micro filtration, Water Res., 35 (2001) 1256–1262.

[33] M.A. Islam, M.R. Uddin, M.S.A. Amin, M.I. Haque, M.S.R. Molla, Design and operation of a photo-cataytic reactor: a study of dye (methylene blue) removal process, J. Chem. Eng., 28 (2013) 41–44.

[34] M. Muruganandham, M. Swaminathan, Photo-catalytic decolourisation and degradation of Reactive Orange 4 by TiO_2-UV process, Dyes Pigments, 68 (2006) 133–142.

[35] C.C. Liu, Y.H. Hsieh, P.F. Lai, C.H. Li, C.L. Kao, Photo-degradation treatment of azo dye wastewater by UV/TiO_2 process, Dyes Pigments, 68 (2006) 191–195.

[36] K. Sahel, N. Perol, H. Chermette, C. Bordes, Z. Derriche, C. Guillard, Photo-catalytic decolorization of Remazol black 5 (RB5) and Procion red MX-5B-Isotherm of adsorption, kinetic of decolorization and mineralization, Appl. Catal. B-Environ., 77 (2007) 100–109.

[37] C. Richard, P. Boule, Photo-catalyic oxidation of phenolic derivatives: influence of $OH^{\cdot}$ and h^+ on the distribution of products, New. J. Chem., 18 (1994) 547–552.

[38] R.B. Draper, M.A. Fox, Titanium dioxide photo-sensitized reactions studied by diffuse reflectance flash photolysis in aqueous suspensions of TiO_2 powder, Langmuir, 6 (1990) 1396–1402.

[39] C. Wei, W.Y. Lin, Z. Zainal, N.E. Williams, K. Zhu, A.P. Kruzic, R.L. Smith, K. Rajeshwar, Bactericidal activity of TiO_2 photo-catalyst in aqueous media: toward a solar-assisted water disinfection system, Environ. Sci. Technol., 28 (1994) 934–938.

[40] J.M. Herrmann, Heterogeneous photo-catalysis: fundamentals and applications to the removal of various types of aqueous pollutants, Catal. Today, 53 (1999) 115–129.

[41] O. Legrini, E. Oliveros, A.M. Braun, Photochemical processes for water-treatment, Chem. Rev., 93 (1993) 671–698.

[42] D. Chen, J. Zhong, Y. Wang, Kinetic study of the photo-catalytic degradation of dye in TiO_2 suspension system, J. Fine Chem., 19 (2002) 55–58.

[43] S. Fassi, K. Djebbar, T. Sehili, Photo-catalytic degegradation of bromocresol green by TiO_2/UV in aqueous medium, J. Mater. Environ. Sci., 5 (2014) 1093–1098.